Journal of Magnetics 17(1), 56-60 (2012) http://dx.doi.org/10.4283/JMAG.2012.17.1.056

Shorted Turn in the Flat Coil Actuator for Fast Initial Response

Ki Il Hwang[1], Tae Won Seo[1], Bongsob Song[2], and Jin Ho Kim[1]*

[1]*Department of Mechanical Engineering, Yeungnam Univertity, Gyeongbuk, Gyeongsan, Daehak-Ro 280, Korea*
[2]*Department of Mechanical Engineering, Ajou University, Suwon 443-749, Korea*

(Received 1 December 2011, Received in final form 14 February 2012, Accepted 15 February 2012)

This paper presents an analysis and experiment of the flat coil actuator with shorted turn. The flat coil actuator is widely used in high precision products because it has no friction between the moving coil and the guide. A shorted turn and a center pole are placed into the flat coil actuator in order to reduce the inductance of the coil and improve the initial response when the actuator is voltage-driven. Enhanced dynamic performance of the flat coil actuator with shorted turn was demonstrated by simulation and experiment.

Keywords : flat coil actuator, shorted turn, lumped parameter analysis, laser interferometer

1. Introduction

The voice coil actuator has received much attention for precision positioning devices because of its quick response, light weight moving parts, easy control with no magnetic attraction and no force ripple [1, 2].

In the early 1980s, the dynamic performance of dual path voice coil actuator was improved by wrapping its center pole with a thin copper plate called by shorted turn. Fig. 1 shows a schematic diagram of shorted turn in dual path voice coil motor. When a voltage is applied to the coil of dual path type motor, the flux in the magnetic circuit induces a high current in the copper sleeve such that it can retard the increase of the magnetic flux. As a result, the inductance of the main coil is reduced and the current rises quickly [3-6].

A flat coil actuator, a kind of voice coil actuator, has merits when used in subminiature products because it has a thin-plate shaped coil, and easy generate linear motion. However, the shorted turn in the flat coil actuator for fast response had not been studied so far.

In this paper the shorted turn used to generate a fast initial response in the flat coil actuator is presented. This approach has not been a case, reported of application to a flat coil actuator. To verify the faster rise of electric coil current due to the shorted turn, a lumped parameter analysis is performed. In addition, the manufactured prototype was tested to demonstrate the enhanced dynamic response of a flat coil actuator due to the shorted turn.

*Corresponding author: Tel: +82-53-810-2441
Fax: +82-53-810-4627, e-mail: jinho@ynu.ac.kr

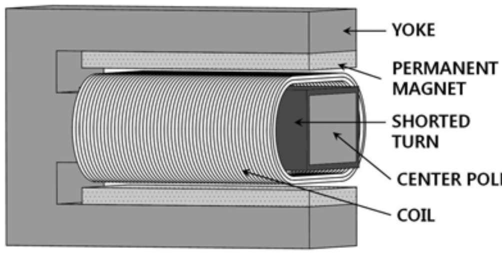

Fig. 1. Schematic diagrams of dual path voice coil motor with shorted turn.

2. Actuator Configuration

Fig. 2(a) shows a schematic diagram of a conventional flat coil actuator. The actuator is composed of a steel yoke, a movable coil in an air gap and permanent magnets that provides a uniform magnetic field in the air gap. When an electric current is passed through the coil, generates a magnetic force. The magnetic force called Lorentz force can be explained by Eq. (1).

$$F = nB_g i l_{eff} \tag{1}$$

The conventional flat coil actuator, however, has a delayed initial response when it is driven by voltage control due to the inductance, which is a typical characteristic of an electromagnetic coil. In the proposed flat coil actuator, to reduce the inductance a steel center pole is inserted

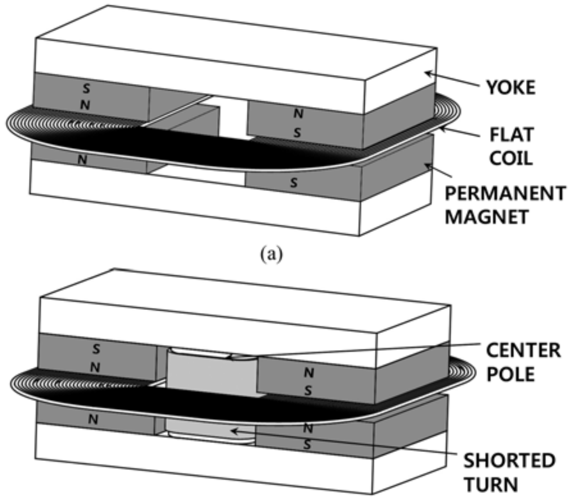

Fig. 2. Schematic diagrams of conventional flat coil actuator (a) and proposed flat coil actuator with shorted turn (b).

between the steel yokes and then wrapped by a thin copper plate to apply the effect of the shorted turn, as shown in Fig. 2(b).

3. Lumped Parameter Analysis

Lumped parameter analysis, an alternative to finite element analysis, is popular for its accuracy and quick computational iterations [7]. To verify the fast rise of electric current in coil due to the shorted turn, lumped parameter models of the conventional actuator without the shorted turn and the new actuator with shorted turn are created respectively.

The coil magnetic flux pattern in the conventional actuator is shown in Fig. 3 which is the cross-sectional 2-D model of Fig. 2(a). The induced Faraday voltage in the coil is presented by Eq. (2) as follows.

$$e = -N\frac{d\Phi}{dt} \quad (2)$$

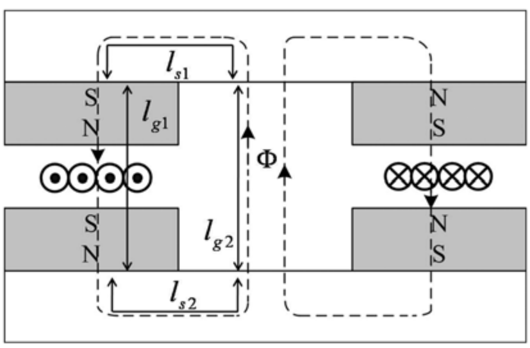

Fig. 3. Lumped parameter model of conventional flat coil actuator.

Table 1. Symbol of lumped parameter analysis of conventional flat coil Actuator.

Symbol	Quantity	Symbol	Quantity
e	Induced voltage in coil	Φ	Mutual flux
N	Number of coil turns	V	Applied voltage source
I	Current in coil	R	Resistance of coil
P	Permeance seen by Φ	L	Inductance seen by P
l_g	Length of air gap	l_s	Length of steel yoke
A_s	Cross section area of steel yoke	A_g	Cross section area of air gap
B_g	Flux density within the air gap	l_{eff}	Effective coil length in the magnetic field for each turn

The applied voltage source and the magneto motive force can be expressed by Eq. (3) and (4) by Kirchhoff's law and magnetic Ampere's law.

$$V = Ri - e \quad (3)$$

$$Ni = \frac{\Phi}{P} \quad (4)$$

3.1. Conventional flat coil actuator

Combining Eq. (4) into Eq. (2) gives Eq. (5), and then the Eq. (5) is combined with Eq. (3) to give Eq. (6). In this model, the coil is assumed to be stationary. In this Eq. (6), the speedance term is neglected. Permeance of the magnetic flux can be expressed by Eq. (8).

The length of air gap 1 includes the lengths of the two magnets and the coil, but the length of air gap 2 is assumed to be the same as the length of air gap1 because of the permeabilities of the magnet and copper, which are quite similar to the permeability of air.

$$e = N\frac{d[PNi]}{dt} \quad (5)$$

$$V = Ri + N\frac{d[PNi]}{dt} \quad (6a)$$

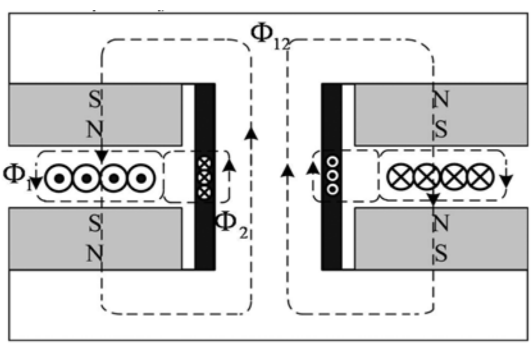

Fig. 4. Lumped parameter model of flat coil actuator with shorted turn.

$$V = Ri + L\frac{di}{dt} \tag{6b}$$

$$L = N^2 P \tag{7}$$

$$P = \frac{\mu_s \cdot A_s}{l_{s1} + l_{s2}} + \frac{\mu_g \cdot A_g}{l_{g1} + l_{g2}} \tag{8}$$

From the Eq. (6), the asymptotic final current value of the conventional flat coil actuator can be expressed by Eq. (9).

$$i_{conventional} = \frac{V}{R} \tag{9}$$

3.2. Proposed flat coil actuator

The magnetic flux patterns of the coil and the shorted turn in the proposed flat coil actuator are shown in Fig. 4.

The transient current flow i_1 in the coil induces a transient current flow i_2 in the shorted turn in the opposite direction. Induced Faraday voltages in the coil and shorted turn, based on Faraday's Law, are presented by Eqs. (10) and (11), respectively.

$$e_1 = -N_1\frac{d(\Phi_{12} + \Phi_1)}{dt} \tag{10}$$

$$e_2 = -N_2\frac{d(\Phi_{12} + \Phi_2)}{dt} \tag{11}$$

The voltage sources of the coil and shorted turn can be expressed by Eqs. (12) and (13) based on Kirchhoff's Law and Ohm's Law, respectively.

$$V_1 = R_1 i_1 - e_1 \tag{12}$$

$$0 = R_2 i_2 - e_2 \tag{13}$$

Table 2. Symbol of lumped parameter analysis of proposed flat coil Actuator.

Symbol	Quantity	Symbol	Quantity
V_1	Applied voltage source	R_1	Coil resistance
R_2	Shorted turn resistance	e_1	Induced voltage in coil
e_2	Induced voltage in shorted turn	N_1	Number of turns in the coil
N_2	Number of turns in the shorted turn	Φ_1	Leakage flux unique to coil only
Φ_2	Leakage flux unique to shorted turn only	Φ_{12}	Mutual flux, linking both coil and shorted turn
i_1	Current in coil	i_2	Current in shorted turn
P_1	Permeance seen by Φ_1	P_2	Permeance seen by Φ_{12}
P_{12}	Permeance seen by Φ_{12}	L_1	Inductance seen by P_1
L_2	Inductance seen by P_2	L_{12}	Inductance seen by P_{12}
l_{coil}	Length of coil	$l_{shorted}$	Length of shorted turn
A_{coil}	Cross section area of Φ_1 path	$A_{shorted}$	Cross section area of Φ_2 path

Table 3. Lumped model parameters.

N	1136 (turns)	N_1	1136 (turns)
N_2	1 (turn)	R	346 (Ω)
R_1	346 (Ω)	R_2	1.062×10^{-4} (Ω)
V	24 (V)	V_1	24 (V)
L	81 (mH)	L_1	9 (mH)
L_2	6.1 (mH)	L_{12}	81 (mH)
B_g	0.674 (Wb/m^2)		

Also, the magneto motive force is expressed by Ampere's law in Eqs. (14), (15) and (16).

$$N_1 i_1 + N_2 i_2 = \frac{\Phi_{12}}{P_{12}} \tag{14}$$

$$N_1 i_1 = \frac{\Phi_1}{P_1} \tag{15}$$

$$N_2 i_2 = \frac{\Phi_2}{P_2} \tag{16}$$

Combining theses equations from Eq. (10) to Eq. (16) comes to Eqs. (17) and (18) [7].

$$V_1 = R_1 i_1 + (L_{12} + L_1)\frac{di_1}{dt} + L_{12}\frac{di_2^*}{dt} \tag{17}$$

$$0 = R_2^* i_2^* + L_{12}\frac{di_1}{dt} + (L_{12} + L_2)\frac{di_2^*}{dt} \tag{18}$$

where, $i_2^* = \frac{N_2}{N_1} i_2$ and $R_2^* = \left(\frac{N_1}{N_2}\right)^2 i_2$.

$$P_1 = \frac{\mu_0 \cdot A_{coil}}{l_{coil}} \qquad L_1 = N_1^2 P_1 \tag{19}$$

$$P_2 = \frac{\mu_0 \cdot A_{shorted}}{l_{shorted}} \qquad L_2 = N_1^2 P_2 \tag{20}$$

$$P_{12} = \frac{\mu_s \cdot A_s}{l_s} + \frac{\mu_g \cdot A_g}{l_g} \qquad L_{12} = N_1^2 P_{12} \tag{21}$$

From Eqs. (17) and (18), the asymptotic final current value of the proposed flat coil actuator can be expressed by Eq. (9).

$$i_{proposed} = \frac{V_1}{R_1 + R_2^*} \tag{22}$$

The parameters of each actuator are shown in Table 3. The sizes of the actuators with and without shorted turn are 100 mm × 50 mm × 45 mm, respectively.

The Eq. (7) and the coupled Eqs. (17) and (18) were solved respectively to obtain the current responses of the conventional flat coil actuator and proposed flat coil

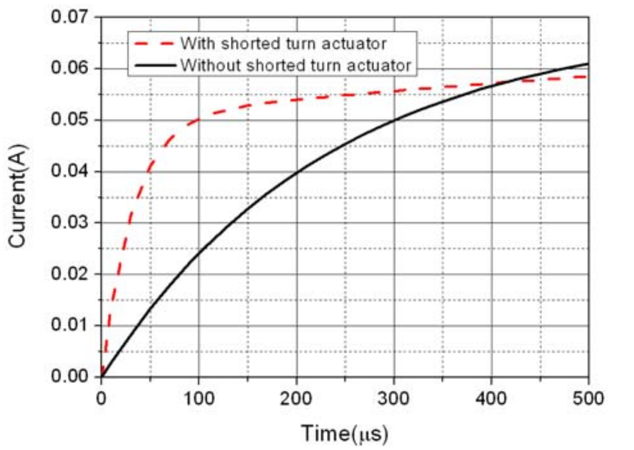

Fig. 5. (Color online) Comparison between models without and with shorted turn respectively, for current of coil versus time by lumped parameter analysis.

actuator with the shorted turn as shown in Fig. 5. The rate of current increase of the proposed flat coil actuator is a few times higher than that of the conventional flat coil actuator in the initial period. However, after 400 microseconds, the current of the conventional actuator becomes higher than that of the proposed actuator because of the differences of the asymptotic final current value.

4. Experiment

To demonstrate the enhanced dynamic response of the flat coil actuator due to the shorted turn, a prototype was manufactured and tested. Two prototypes of the flat coil actuator, one without a shorted turn and the other one with a shorted turn, were manufactured. The moving coil type actuators, whose coil motion was guided by the leaf spring, were fabricated, as shown in Fig. 6. The total moving mass is 140 g and the total stiffness of leaf springs is 5.46 N/um.

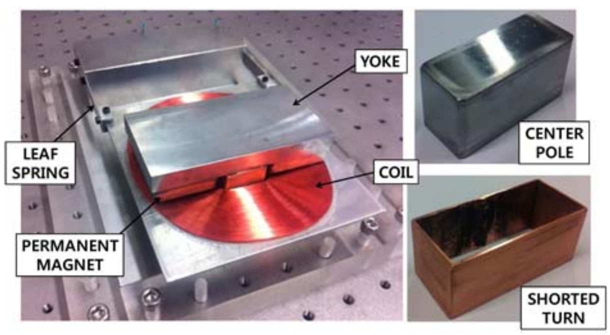

Fig. 6. (Color online) Prototype of flat coil actuator using shorted turn and simple linear guide.

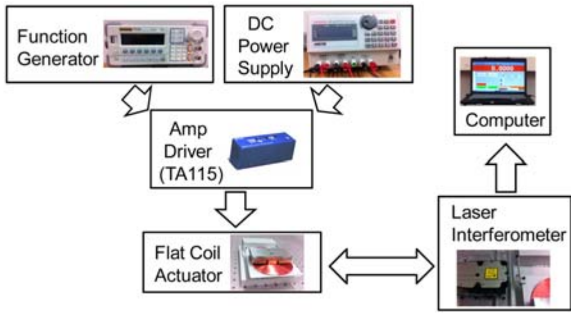

Fig. 7. (Color online) Schematic diagram of experimental setup.

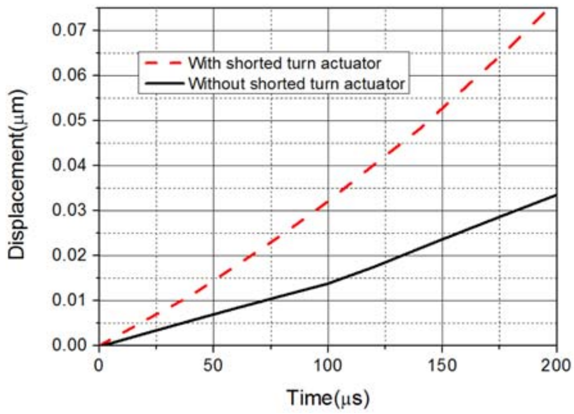

Fig. 8. (Color online) Comparison between models without and with shorted turn respectively, for displacement of coil versus time by experiment.

Fig. 7 shows the experiment setup including a function generator, DC power supply, the linear amp driver, laser interferometer and personal computer. With DC power supply, the square wave of 24 Volts was applied to the coil and the position of moving coil versus time was measured with the laser interferometer during 200 μs which is ordinary period of actuator control. The actuator was installed on the air vibration isolation table to prevent the noise due to external vibration.

5. Result

Fig. 8 shows the measured results. The displacement of the actuator with the shorted turn was 0.077 μm during 200 μs whereas one without the shorted turn was 0.034 μm: the velocity of coil was improved by 2.3 times due to the faster initial current response with the shorted turn. In the lumped parameter model, the coil is assumed to be stationary; therefore the speedance term is neglected. On the other hand, the coil in the experiment is moving according to the time; therefore the speedance term exists.

6. Conclusion

The shorted turn in a flat coil actuator proposed to achieve initial fast response was investigated. The lumped parameter analysis verified the faster rising current due the shorted turn and the experiment with a manufactured prototype demonstrated the two-fold enhanced dynamic response during the initial period.

Acknowledgement

This research was supported by Yeungnam University research grant in 2011.

References

[1] M. Hiyane, Y. Inoue, and M. Kurusu, Fujitsu Scientific and Technical Journal, **2**, 59 (1972).
[2] H. Shinno and H. Hashizume, CIRP Annals-Manufacturing **50**, 243 (2001).
[3] J. Arthur Wagner, IEEE Trans. Magn. **18**, 1770 (1983).
[4] Y. Hirano, J. Naruse, and R. Tsuchiyama, IEEE Trans. Magn. **25**, 3073 (1989).
[5] C. Dong, IEEE Trans. Magn. **19**, 1689 (1983).
[6] T. S. Liu and C. W. Yeh, IEEE Mediterranean Electrotechnical Conference 1153 (2010).
[7] J. P. Wang, D. K. Lieu, W. L. Lorimer, and A. Hartman, IEEE Trans. Magn. **33**, 4092 (1997).